Non-adiabatic simulations of current-related structural transformations in metallic nanodevices

2011 J. Phys.: Condens. Matter 23 345301

(http://iopscience.iop.org/0953-8984/23/34/345301)

IOP PUBLISHING JOURNAL OF PHYSICS: CONDENSED MATTER

J. Phys.: Condens. Matter **23** (2011) 345301 (9pp) doi:10.1088/0953-8984/23/34/345301

Non-adiabatic simulations of current-related structural transformations in metallic nanodevices

M Todorović[1,5] **and D R Bowler**[2,3,4]

[1] Departamento de Física Teórica de la Materia Condensada, Universidad Autónoma de Madrid, E-28049 Madrid, Spain
[2] Department of Physics and Astronomy, University College London, Gower Street, London WC1E 6BT, UK
[3] Thomas Young Centre, University College London, Gower Street, London WC1E 6BT, UK
[4] London Centre for Nanotechnology, 17-19 Gordon Street, London WC1H 0AH, UK

E-mail: milica.todorovic@uam.es

Received 9 June 2011
Published 12 August 2011
Online at stacks.iop.org/JPhysCM/23/345301

Abstract

One of the less explored aspects of molecular electronics is the effect of current on the mechanical stability of the conducting molecule: charge flow can alter both the geometry and electronic properties of the device, modifying the conductance and giving rise to nonlinear conduction characteristics or conductance switching. We performed a fundamental study on the correlation between the geometry and evolving electronic structure of small Au clusters that were embedded in finite Au wires and subjected to periodic transient currents. Both the current-carrying electronic states and the local electronic structure of the model system were described away from the ground state within a time-dependent Ehrenfest formalism. Non-adiabatic molecular dynamics simulations revealed that clusters undergo structural transformations between several representative geometries that coincide with patterns in cluster charging. The shape changes were enabled by the fluctuations in cluster band filling associated with the current and assisted by current-related forces. Metastable configurations of stable clusters were linked to events of charge trapping on the cluster.

(Some figures in this article are in colour only in the electronic version)

1. Introduction

Measurements of molecular conductance in recent years have captured several examples of nonlinear conduction behaviour, such as conductance switching [1–3] and negative differential resistance [4, 5]. These observations signal a departure from the elastic tunnelling electronic transport regime, but remain difficult to interpret [6]. A better understanding of inelastic electronic tunnelling spectroscopy (IETS) measurements is frustrated by their sensitivity to experimental configuration and impurities, which make it difficult to clearly identify the features of inelastic electronic transport regimes. For example, in cases where changes in molecular geometry were also reported [1], there is little evidence to indicate whether molecular motion gives rise to the complex conduction characteristics or results from them.

Few theoretical conductance studies consider structural instability, since standard calculation methods widely assume that conducting molecules retain their ground-state geometry. This is a reasonable approximation in the case of low current density and elastic electronic transport, but the coupling between molecular structure and electronic states is often not negligible [7]. Prospective mechanisms of molecular motion such as vibrational modes, polaronic distortions and electromigration are well understood, but rarely studied dynamically and in the presence of electrical current. Electromigration has yet to be explored in molecular systems,

[5] Work carried out at: Department of Materials, University of Oxford, Parks Road, Oxford OX1 3PH, UK.

although it was shown that it can weaken local bonding in solid-state nanostructures: depending on current density, it can lead to mechanical failure [8, 9] or structural rearrangement accompanied by changes in conductance properties [10].

This study aims to explore the response of generic nanostructures to current, in terms of both their mechanical stability and their electronic properties. We set out to characterize the basic mechanisms of interaction between charge flow and conducting structures. Development of methods for dynamical study of nanoscale conduction, with currents explicitly included, is central to our investigation.

The dearth of studies on the dynamics of molecular conduction is largely due to the lack of suitable theoretical frameworks. The Landauer–Büttiker theory [11] coupled with the non-equilibrium Green's function (NEGF) approach [12] has been enormously successful in describing steady-state conduction properties of static molecular structures, but cannot tackle dynamic or transient conduction effects (short-term response of molecules) such as molecular charging, conformation switching, current-triggered molecular vibrations or related Joule heating. Electron–phonon interactions can be included as perturbations to elastic electronic transport through the self-consistent Born approximation [13], but the limits of the perturbative regime are system dependent and often unclear. Most dynamical methods, on the other hand, rely on the Born–Oppenheimer approximation and are unable to account for non-adiabatic current-carrying electronic states or their dependence on external bias [14]. Moreover, they lack the mechanism for energy exchange between the electronic states and vibrational modes of the atomic system that is fundamental to current-triggered phenomena. In theory, such energy transfer can be exploited to drive useful molecular motion through the action of a non-conservative force induced by electronic currents [15, 16].

Bridging this gap are time-dependent semi-classical methods based on the mean-field approximation. Here, single electron eigenstates are evolved using the Ehrenfest expression in parallel to the atomic equations of motion (EOM). Depending on the form of the Hamiltonian and basis functions, the Ehrenfest formalism has been coupled with different electronic structure methods ranging from density-functional theory (DFT) [17, 18] to tight-binding approaches [19, 20]. The time-dependent tight-binding framework (TDTB) is non-perturbative and can be manipulated to accommodate bias voltage and generate charge flow [21], making it a useful tool for dynamical studies of conduction (alongside time-dependent density-functional theory, TDDFT, and its current-density formulation [22, 23]). The simplicity and transparency of TB interactions is particularly suited to studies of model systems, although computed conduction properties of simple molecular junctions were shown to exhibit also quantitative agreement with NEGF calculations [24]. Lastly, atomic forces in the TDTB model implicitly contain bias-voltage dependence, which makes it possible to identify current-induced force contributions [25, 10] and study current-related effects in conducting nanostructures.

In this paper, we applied TDTB to molecular dynamics simulations of a simplified molecular junction. The system featured small metallic clusters embedded in finite single-line wires, that served as charge reservoirs. Non-adiabatic treatment of electronic states made it possible to set up permanent charge waves in the leads and imitate transient currents. In the molecular dynamics simulations that followed, we monitored the geometry and electronic structure of the metallic clusters in order to explore the response of the structure to charge flow. All clusters exhibited similar current-driven behaviour, involving structural transformations and particular charge states. The structural energy difference theorem (SEDT) [26] can be used to predict the change in relative stability of simple structures with band filling by considering their band energy. We applied it to isolated clusters, then used this information to interpret the link between cluster charge and shape during molecular dynamics simulations and understand the mechanism of structural transformations.

In section 2 of this paper, we discuss features of the model system and the application of the TDTB framework to non-adiabatic molecular dynamics simulations. We also describe how the SEDT was used to explore the relation between cluster band filling and its geometry. Results of non-adiabatic molecular dynamics and the range of observed effects are presented in section 3, while section 4 contains the interpretation and analysis of cluster behaviour. Our findings are summarized in section 5, and we conclude by relating this simple study to molecular conduction properties.

2. The methodology

2.1. The non-adiabatic electronic structure formalism

The derivation of the TB Ehrenfest framework used in this study is published elsewhere [20, 21], but here we restate the important characteristics of the model and discuss the nature of the resulting non-adiabatic molecular dynamics simulations. The atomic and electronic subsystems are entirely described by the set of atomic positions $\mathbf{R}_n(t)$ and the electronic density matrix $\mathbf{\Omega}(t)$ respectively. These quantities are evolved in time concurrently and consistently, using the non-adiabatic equations of motion below:

$$M_n\ddot{\mathbf{R}}_n(t) = -2\sum_{n'\neq n}\mathrm{Re}\,[\Omega_{n'n}]\nabla_n H^0_{nn'} - \nabla_n\varepsilon^{\mathrm{TB}} - \nabla_n V^{\mathrm{TB}} \quad (1)$$

$$\mathrm{i}\hbar\dot{\mathbf{\Omega}}(t) = [\mathbf{H}^{\mathrm{TB}}(t), \mathbf{\Omega}(t)]. \quad (2)$$

System Hamiltonian $\mathbf{H}^{\mathrm{TB}}$ is defined below in (4). V^{TB} describes the repulsive atomic interaction energy in the TB form of pair potentials, and ∇_n is a vector differential operator with respect to the position of atom n. Charge self-consistency of the model was imposed through the electrostatic potential energy $\varepsilon^{\mathrm{TB}}$. Both the on-site and the inter-site electrostatic terms were included in the model to improve the accuracy of the charge transfer and the description of electronic current, as detailed in (3). Here, Δq_n is Ω_{nn} and describes net excess of electrons on an atom, or charge transfer, which is regulated by the atomic on-site and inter-site Coulomb parameters U_n and $u_{nn'}$. Atomic charging was relatively insensitive to parameter

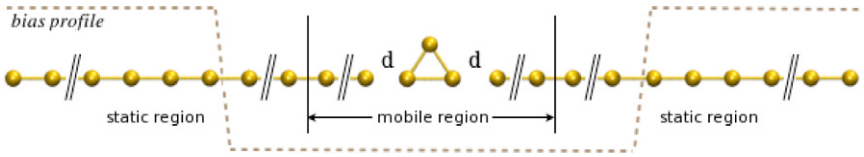

Figure 1. Schematic diagram of the conducting system featuring the Au_3 cluster (101 atoms). Diagonal lines replace the remaining length of the leads. Only ten innermost atoms in each lead are mobile, while 25 outermost atoms in each lead feature high bias potential, as described by (5). The initial cluster–lead distance is d.

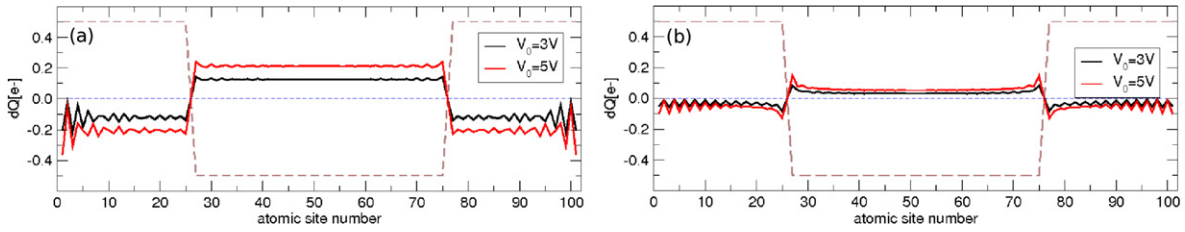

Figure 2. Distribution of electrons in a linear wire of 101 atoms with an external bias potential multiplied by a bias amplitude V_0 of 3 and 5 V: (a) without charge self-consistency; (b) with charge self-consistency. The shape of the external potential is shown by a dashed line.

values so these were set to 7 eV for all atoms and pairs of atoms in a compromise between lack of self-consistency ($U = 0$) and local charge neutrality ($U = \infty$). The charge self-consistency potential U^{TB} was added to the diagonal elements of the purely TB Hamiltonian matrix $\mathbf{H}^0$, thus generating the full Hamiltonian $\mathbf{H}^{\mathrm{TB}}$ that was used in the evolution of electronic states through (2):

$$\varepsilon^{\mathrm{TB}} = \tfrac{1}{2}\sum_n U_n \Delta q_n^2 + \tfrac{1}{2}\sum_n \sum_{n' \neq n} u_{nn'} \times \Delta q_n \Delta q_n' / |\mathbf{R}_n - \mathbf{R}_{n'}| \tag{3}$$

$$H_{nn'}^{\mathrm{TB}} = H_{nn'}^0 + U_{nn'}^{\mathrm{TB}} = H_{nn'}^0 + \delta_{nn'}\left(U_n \Delta q_n + \sum_{n'' \neq n} u_{nn'} \Delta q_n'' / |\mathbf{R}_n - \mathbf{R}_{n'}|\right). \tag{4}$$

The test system was simulated by an s-band TB scheme for Au [27] that was previously used in studies of electromigration [10] and current-related effects [24, 15]. The simplicity of the TB interaction model lends further transparency and physical meaning to the simulations. Details of the scheme can be found in the appendix of this paper.

The advantage of deriving the Hellmann–Feynman force [28] shown in (1) through the system Lagrangian [20] is that the Pulay forces arising from the time dependence of the electronic basis set [29, 30] are automatically included in the electronic structure force contribution. In the presence of current, the same term also contains the non-adiabatic force that arises from the bias-voltage dependence of the electronic density matrix, i.e. the bias-related change in the population of the left and right travelling current-carrying electronic states [31, 25].

2.2. The model nanocircuit

The TDTB formalism outlined above was applied to an elementary nanocircuit model in which small clusters were attached to finite linear electrodes. The leads were also reservoirs of charge, which was manipulated to induce charge waves across the entire length of the system. Our aim was to study the effect of this current on the central cluster. In order to maximize the period of charge flow induced across the cluster but keep simulation costs low, 49 atoms were included in each linear electrode, making the system size just over 100 atoms. The characteristic bond length in the leads was set to the equilibrium bond length calculated for an infinite linear Au chain [27]. Since the primary purpose of the leads was to host the current, only ten atoms in each lead that were closest to the cluster were allowed to move and accommodate cluster dynamics. Figure 1 shows an example of the entire conducting system.

In this closed system (free boundary conditions), a biasing potential described in the following equation was added to the diagonal Hamiltonian matrix elements at time $t < 0$:

$$V_n^{\mathrm{bias}} = \begin{cases} +0.5V_0 & n \leq 25, \quad N - 25 \leq n \\ -0.5V_0 & 25 < n < N - 25. \end{cases} \tag{5}$$

Here, N is the total number of atoms in the system and V_0 is the magnitude of the potential in volts. The effect of the bias potential on the system charge distribution with and without charge self-consistency is shown in figure 2. It demonstrates the tendency of the charge self-consistent model to delocalize charge and thus reduce charge transfer. The bias potential was removed immediately before the start of non-adiabatic simulations, giving rise to two opposite charge wavefronts that traverse the entire system and reflect back at the ends of the electrodes. Like all atoms, the central cluster was thus periodically charged and discharged, the varying population of the cluster anti-bonding orbitals being equivalent to transient currents traversing the cluster. The voltage magnitude and shape of the bias potential were selected empirically to keep cluster charging low and control its timing.

The initial bias potential perturbation of electronic states was translated into an electrical current by propagating

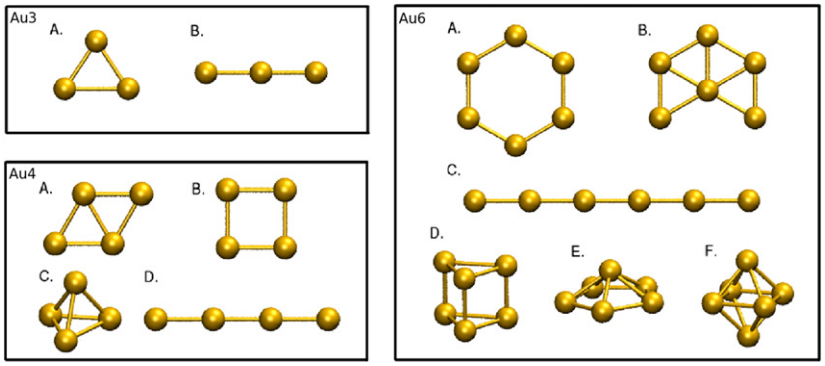

Figure 3. Regular geometries of Au_N clusters compared in SEDT calculations. Au_3: (A) triangle, (B) linear shape; Au_4: (A) rhombus, (B) square, (C) tetrahedron, (D) linear shape; Au_6: (A) hexagon, (B) concave hexagon, (C) linear shape, (D) triangular prism, (E) hexahedron, (F) octahedron.

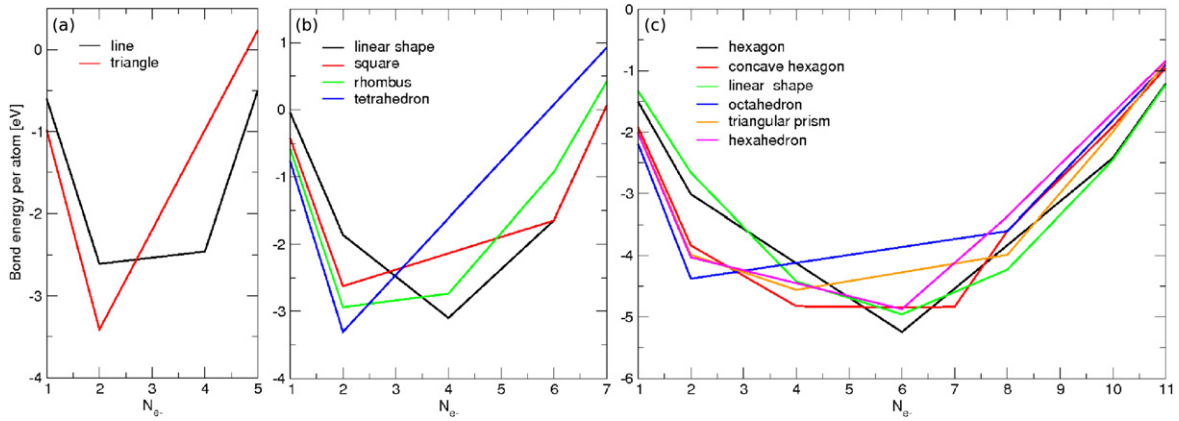

Figure 4. Bond energy per atom of a Au_N cluster as a function of the number of electrons on the cluster (band population): (a) Au_3; (b) Au_4; (c) Au_6.

electronic states via the Ehrenfest formalism in (2). The substantial reduction in computational time gained by removing Hamiltonian diagonalizations was partially offset by the increased number of iterations required with a molecular dynamics time step of 10^{-17} s. As band occupation of the original biased Hamiltonian was preserved, the electronic system was kept away from the ground state of the instantaneous Hamiltonian at all times. The corresponding inability to visit specific excited states of the system is a well-known consequence of the mean-field Ehrenfest approach, that is addressed by other techniques such as surface hopping [32, 33]. The mean-field approximation is also responsible for the averaging of energy and momentum transfers from electrons to ions, making it impossible to reproduce Joule heating [34, 35]. This effect is relevant to conduction of some nanostructures [36, 37], but should not affect our study at low voltage and temperature. Correction terms can be employed to include heating effects into the model [38] but are not considered here.

2.3. The structural energy differences theorem analysis

In an attempt to interpret any shape changes of conducting clusters during molecular dynamics simulations, we explored the relative stability of different cluster geometries. Small clusters that can take a limited number of simple geometries make it easy to identify changes in their physical and electronic structure, so we considered clusters of three, four and six Au atoms with the geometries shown in figure 3. All geometries are regular and can be described by a single bond length a. The three-atom cluster Au_3 is the smallest structure with non-trivial geometry and the ideal test system, although Au_4 and Au_6 both feature a relatively small number of available geometries.

The SEDT [26] was used to explore the energetics of cluster band filling, which is roughly equivalent to cluster charging (which also involves small electrostatic energy contributions). Its practical application involved adjusting the characteristic bond length for each geometry type until their repulsive potential energies were the same, and then computing a series of energy points for different charged states of the cluster. The variation in bond energy with charge was plotted to obtain the structural stability charts shown in figure 4, and thus identify the favoured geometry of a charged structure. A cluster with half-filled bands was defined as neutral. Low-coordination (linear and circular) shapes consistently exhibited lowest energies if the clusters were neutral or negatively charged. In contrast, clusters with low band filling and positive net charge favoured high-coordination two-dimensional geometries (such as triangular or rhomboid shapes). The computed stability trends agree with the behaviour expected from analytic model

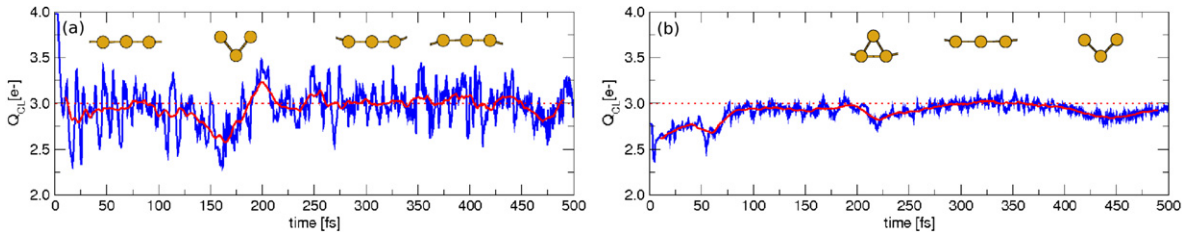

Figure 5. Number of electrons on the Au_3 cluster as a function of simulation time, with a running average over 10 fs superimposed. Important instantaneous geometries are shown. The cluster was initially a regular triangle with $a = 3$ Å, the cluster–lead separation was $d = 4$ Å and the potential well bias profile was used with (a) $V_0 = 5$ V in the charge non-self-consistent case and (b) $V_0 = 3$ V in the charge self-consistent case.

calculations [26]. We might expect cluster band occupation to vary in the presence of current, but only within ± 1 e^- given the weak charge waves. This suggests that clusters may switch between linear and intra-bonded geometry types if their charge oscillates around the neutral value.

While the SEDT supplies a straightforward and fundamental link between cluster charge and shape, it only takes regular geometries into consideration. Through structural optimizations, we identified and catalogued several distorted cluster geometries that compete for stability with regular structures and share their bond coordination characteristics. The number of alternative geometries increases with cluster size.

2.4. System variables for non-adiabatic molecular dynamics

Preparation of the conducting system for molecular dynamics involved setting initial conditions for both the cluster geometry and biased charge distribution. Geometries favoured by neutral and singly charged clusters were chosen for initial cluster configurations. Unless the initial cluster geometry was linear, a cluster–lead separation d was adopted to allow space for any further geometry transformations. In order to also explore the effect of device–lead coupling strength on cluster behaviour, we varied d typically between 3.5 and 5 Å in steps of 0.5 Å while making sure to maintain orbital overlap between the cluster and leads. With each set of initial conditions we performed molecular dynamics simulations with and without charge self-consistency, so as to determine the role of different charge treatments for the current and cluster conduction. The potential magnitude V_0 was set to 5 V in charge non-self-consistent simulations, and 3–5 V otherwise (to reduce atomic charging and avoid charge front delocalization through inter-site electrostatic repulsion). We removed thermal fluctuations of the conducting system for clarity by assigning no initial or thermal velocities to ions.

A reference for cluster motion under charge flow was established by performing molecular dynamics simulations of the neutral and singly charged clusters in isolation. When the initial shape of the cluster corresponded to its charge, only breathing oscillations of structures were observed and cluster shape was preserved. In other cases, clusters underwent continuous transformations, oscillating between the initial shape and the one more closely associated with given cluster charge. The observations suggested that an initial mismatch in cluster charge and geometry introduces an amount of excess energy into the system which can lead to cluster dissociation, unless cluster bond lengths are adjusted.

3. Results from non-adiabatic molecular dynamics

Using the range of initial conditions outlined above, we performed a series of non-adiabatic molecular dynamics simulations with the Au_3, Au_4 and Au_6 clusters in order to characterize their response to current. Given a time step of 0.01 fs and total simulation time of 0.5 ps, each calculation took up to a few hours on a single 2.8 GHz desktop workstation. We monitored the band filling of the cluster through its total charge. For example, the presence of charge waves was confirmed by observed rapid oscillations of cluster charge consistent with the length of the leads. The oscillation period of 9 fs indicated an electronic velocity of 3×10^6 m s^{-1}, which agrees with the Fermi velocity in Au.

We analysed the simulations selectively, keeping only those featuring stable clusters, whose dynamics was unrestricted by the leads. Also, some cases of trivial cluster dynamics were not considered: if the starting cluster geometry was favoured by the initial cluster charge, only breathing oscillations of clusters were observed in analogy to isolated cluster dynamics. Similarly, clusters that were initially in linear conformations remained linear unless small velocities were selectively imparted to cluster atoms to excite transverse oscillation modes (which was purposely avoided). The behaviour of clusters in the remaining cases is described below.

3.1. Au_3 cluster dynamics

The simple three-atom cluster has only two regular geometries, triangular and linear, roughly associated by SEDT with underfilled bands and neutral clusters respectively. A typical example of total cluster charge evolution throughout molecular dynamics is plotted in figure 5. In the charge non-self-consistent case, the cluster transforms from the initial triangular form into a linear one within the first 50 fs as the cluster charge returns to the neutral state. At 150 fs, the cluster becomes triangular again and loses about 0.5 e^-, before returning to an uncharged linear configuration where it remains with slight fluctuations for the remainder of the simulation. With charge self-consistency in the model, the

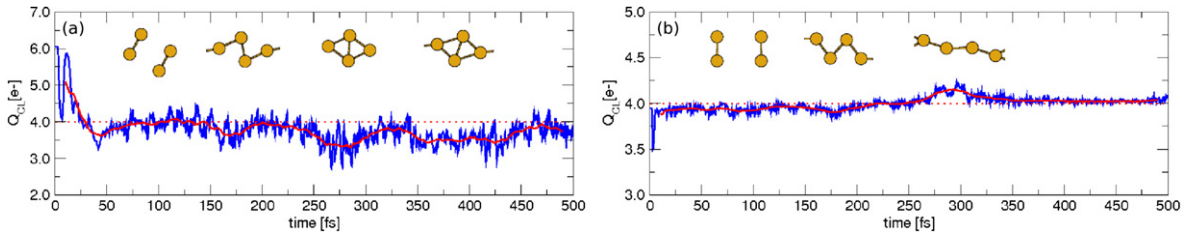

Figure 6. Number of electrons on the Au_4 cluster as a function of simulation time, with a running average over 10 fs superimposed. Important instantaneous geometries are shown. The cluster was initially a relaxed rhombus structure with bonds stretched by 10%, the cluster–lead separation was $d = 3.5$ Å and the potential well bias profile was used with (a) $V_0 = 5$ V in the charge non-self-consistent case and (b) $V_0 = 5$ V in the charge self-consistent case.

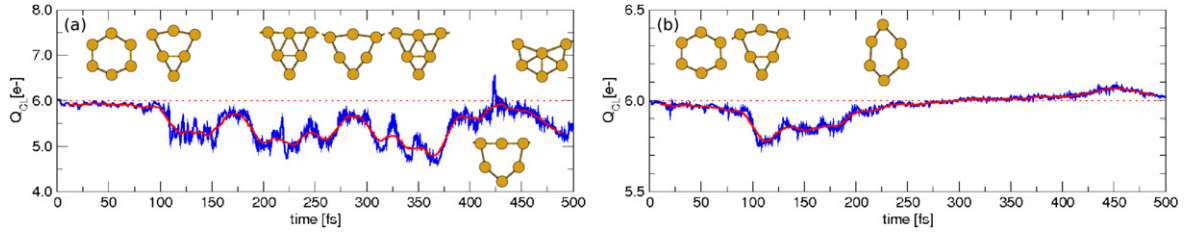

Figure 7. Number of electrons on the Au_6 cluster as a function of simulation time, with a running average over 10 fs superimposed. Important instantaneous geometries are shown. The cluster was initially a relaxed concave hexagon, the cluster–lead separation was $d = 4$ Å and the potential well bias profile was used with (a) $V_0 = 5$ V in the charge non-self-consistent case and (b) $V_0 = 3$ V in the charge self-consistent case.

cluster first returns to triangular form after 200 fs, then again at 450 fs, each time with a slight positive net charge on the cluster. At other times, the cluster is linear and approximately neutral.

Overall, we found that cluster charging was characterized by rapid oscillations indicating currents, but also occasional charge retention of up to 0.5 h^+ that can occur over long timescales. Even though it was affected by initial conditions, cluster charging occurred arbitrarily and was always associated with a hole charge. At other times during the simulation, the cluster was neutral on average and in linear form. Structural transformations between the triangular and linear cluster shapes associated with cluster charging events were clearly observed.

Given similar initial conditions, the charge self-consistent approach altered atomic trajectories, but did not change the qualitative behaviour of the cluster. Smaller cluster charge oscillations reflected the smaller bias-voltage magnitude (3 V), as seen in figure 5(b), but cluster charging was observed nonetheless, accompanied by structural transformations.

3.2. Au_4 cluster dynamics

The conduction behaviour of the four-atom cluster showed many similarities to that of the three-atom cluster. Clusters continued to retain positive charge, as illustrated in figure 6, where about 0.5 h^+ was gained at a time as the cluster oscillated between rhomboid, square and linear geometries. In agreement with SEDT, neutral clusters kept close to a linear conformation, while cluster charging coincided with transformations to a rhomboid form. Although initial cluster states also included negatively charged rhomboids and positively charged squares, similar behaviour was observed. Charge self-consistent simulations featured lower voltage and reduced cluster charging but the correlation between cluster shape and charge persisted.

3.3. Au_6 cluster dynamics

Regular geometries were used as initial conformations for the six-atom cluster in molecular dynamics simulations although a range of stable irregular shapes were identified. As with smaller linear clusters, regular hexagons proved very stable against charge waves. Starting the molecular dynamics simulations with negatively charged concave hexagons (see figure 1 for geometry reference) resulted in lively cluster dynamics and the tendency to retain positive charge. Figure 7 conveys a representative example of cluster charge behaviour throughout simulations with and without charge self-consistency.

Six-atom clusters appear to charge abruptly, take on more significant charge (up to 1 h^+) and retain it for longer periods than smaller clusters. The amount of partial charge indicates that the fractional charge per atom of about 0.2 h^+ remains approximately constant, regardless of cluster size. The charging was accompanied by structural transformations between geometries that were clearly associated with particular charged states, but were not previously identified. Shown in figure 7, these structures nonetheless feature the bond coordination type that agrees with SEDT predictions. Neutral clusters took on low-coordination geometries (a deformed pentagon or hexagon), while positively charged ones formed highly coordinated aggregate triangular structures, as well as concave

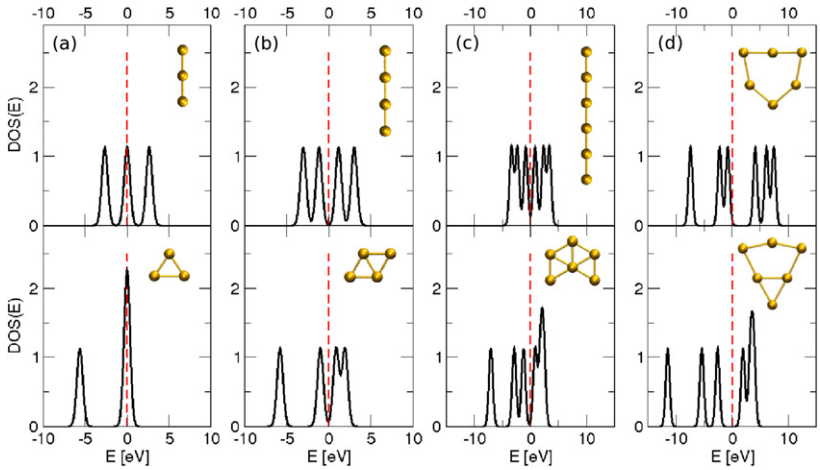

Figure 8. Density of states associated with different bond coordination of the (a) Au_3 cluster, (b) Au_4 cluster, (c) Au_6 cluster and (d) irregular Au_6 clusters featured in non-adiabatic MD. The Fermi level is indicated by a dashed line.

hexagons. Charge self-consistency delocalized charge and thus considerably reduced the amount of net charge retained by the clusters as well as the frequency of cluster charging, but the cluster behaviour remained the same.

4. Discussion

Throughout the molecular dynamics simulations, otherwise neutral clusters were repeatedly found to retain fractions of positive charge over variable time periods (up to 0.1 ps). Moreover, clusters underwent structural transformations between a small number of well-defined geometries. The transformations coincided with periods of cluster charging and discharging, establishing a clear link between particular geometries and band filling of the cluster. The correlation between cluster shape and charge agreed with the predictions of SEDT. As cluster size increases, so does the range of observed structures, but general characteristics persist: neutral clusters are characterized by linear or ring geometries, while positively charged ones feature highly coordinated, intra-bonded geometries.

In order to explain this correlation, we examine and contrast the detailed electronic structure of clusters within the two categories. Topologically, the positively charged structures of the Au_3, Au_4 and Au_6 clusters are composed entirely from three-membered rings, which points to a non-zero third moment μ_3 [39] of their electronic structure (the third moment corresponds to closed three-hop electron paths, summed over all such paths from a single atom, and over all atoms). Since structures with non-zero third moments exhibit a skewed density of states (DOS), we compare the density of states for the neutral and charged geometry types of Au_3, Au_4 and Au_6 clusters in figure 8. The DOS of all neutral cluster geometries is symmetric about the Fermi level, as opposed to the skewed spectrum of the positively charged structures which is biased towards lower energy values. Similar features are evident in the DOS of irregular Au_6 cluster shapes observed in molecular dynamics simulations (figure 8(d)). The shift to lower energies in the eigenstates of intra-bonded geometries indicates that, at low band filling, such structures are more stable than those with symmetrical DOS. Thus intra-bonded geometries are associated with positive cluster charge. As bands are filled further, the energy balance shifts near the Fermi level in favour of low-coordination structures.

The similar cluster behaviour in simulations with and without charge self-consistency arises from the comparable fluctuations in cluster band filling with charge flow. To explore the effects of charge self-consistency without the complicated current-related response of the system, we removed the initial bias in non-adiabatic simulations of the triangular Au_3 cluster system. The initial charge configuration was now the natural ground-state charge distribution, featuring a slight charge separation with an excess of electrons in the leads. Figure 9(a) shows that, without charge self-consistency, this charge distribution persists throughout the simulation and the cluster net charge of approximately 1 h^+ remains constant. No structural transformations were observed. In charge self-consistent simulations, on the other hand, long-range electrostatic interactions across the entire system caused a shift of charge to smooth out the charge separation. A weak charge wave was induced after 300 fs, revealed by small-period oscillations of total cluster charge (see figure 9(b)), that led to cluster charge retention and corresponding changes in geometry. We found that in all of our non-adiabatic simulations, charge self-consistency affected the charge distribution and its evolution through a tendency to suppress charge separation and smear out charge, but did not alter qualitatively the effects of the charge wave on clusters.

The test simulation without bias voltage suggests a stable cluster charge and geometry in the absence of charge waves and varying band population (the same occurs at low voltage). But this was not the only condition for cluster stability: biasing the charge distribution so that cluster charge correlates with its starting geometry did not lead to any charging or structural transformations despite a resulting current. A biased initial charge distribution introduced an

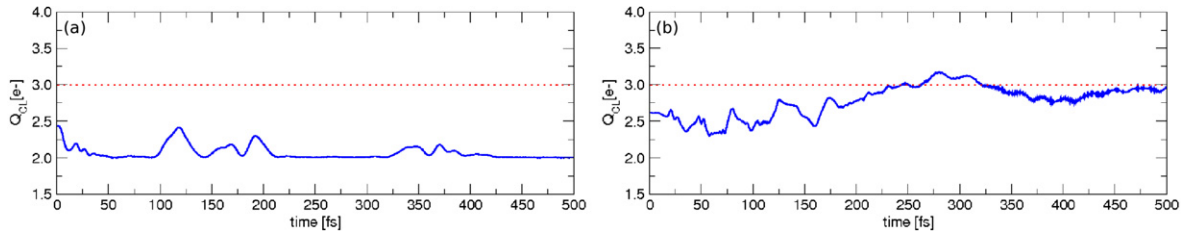

Figure 9. Number of electrons on the Au_3 cluster as a function of simulation time in a simulation without the bias potential. The cluster was initially a regular triangle with $a = 3$ Å and the cluster–lead separation was $d = 4$ Å in both the (a) charge non-self-consistent case and (b) charge self-consistent case.

amount of excess energy into the electronic system. When the initial cluster shape and charge were incompatible, forces on the cluster were large and velocities rose as part of this energy was transferred to cluster atoms, setting off structural transformations throughout the simulation. Alternatively, when the initial cluster shape and charge were congruent, energy was slowly transferred over to all atoms in the system through current-induced forces, with the cluster geometry comparatively stable. We conclude that both the excess energy of the current-carrying states and the directional way in which it was transferred between the electronic and atomic system were necessary conditions for observing structural transformations, regardless of cluster size.

In all simulations we found that Au clusters with underfilled bands stabilized over extended periods of time, while negative charge retention on linear clusters was rare. The SEDT study predicts the hole-charged cluster to be the single most stable cluster state in general, but the observed effect might also arise from the nature of our electrodes: SEDT suggests that linear leads are electron-withdrawing, which was confirmed by the ground-state charge distribution. Most molecular conduction studies oversimplify the electrodes to trivial sources of charge and dissipation, but atomic scale leads such as conjugated polymers or metallic wires may interact with small molecular devices and alter their conduction properties (regardless of the nature and quality of the molecule–lead contact). Lastly, we observed a strong correlation between cluster charge and shape, yet cannot argue that either property determines the other. It is when fluctuations in band occupation coincide with particular structural fluctuations that atomic forces on the cluster become small and appropriate structures are stabilized. In that sense, the non-adiabatic transient current provides the mechanism for structural transformations. This might not be the case with a steady-state current, where the imbalance between left and right travelling states is fixed, keeping the occupation of cluster anti-bonding states roughly constant. Nonetheless, transient currents are important in many experimental studies, and our results indicate that the response of nanoscale systems to voltage pulses and unstable currents might be significant.

5. Conclusions

The Ehrenfest molecular dynamics simulations of small Au clusters (three, four and six atoms) performed in this study explored how transient currents affect cluster stability. We found that clusters undergo structural transformations throughout the simulations, regardless of cluster size. No changes in cluster geometry were observed in the absence of current. Structural transformations coincided with changes in cluster charge, establishing a direct correlation between cluster shape and charge. Charge self-consistent treatment of electronic states affected charge wave properties by smearing out atomic charges in general, but did not alter the qualitative behaviour of clusters.

The link between cluster band filling and structure agrees with predictions of the structural energy difference theorem, and can be explained through the third moment μ_3 of the cluster geometries. Structures with a non-zero third moment (consisting of three-membered rings) have a skewed DOS that promotes their stability at low band filling. Structural transformations were triggered when fluctuating cluster charge, varied by the charge wave, became congruent with its geometry. This observation highlights the importance of the transient current regime, which is relevant in much experimental work. Changes in cluster geometry were assisted by a directional transfer of energy from the current-carrying states to the atomic subsystem via current-induced forces. Despite the simplicity of our model, it was possible to observe these subtle conduction effects by using the non-adiabatic electronic structure formalism. Further research into the current-related energy transfer between electronic and atomic subsystems in conducting nanostructures would enhance our findings, while simulations of more realistic systems in the transient current regime are necessary to relate them to experimental data. Much new physical insight can be gained from dynamical conduction simulations that are now made possible by the range of time-dependent modelling techniques.

Acknowledgments

The authors thank Professor A P Sutton for guidance and support, Dr T N Todorov and Dr C G Sánchez for valuable discussions, and Professor D G Pettifor for the use of computational facilities at the Materials Modelling Laboratory at the Department of Materials, University of Oxford. This study was funded by the Scatcherd European Scholarship awarded by the University of Oxford. DRB is supported by the Royal Society.

Table A.1. Tight-binding parameters for Au [27].

ϵ (eV)	C	a (Å)	$r_{\rm cut}^{\rm in}$ (Å)	$r_{\rm cut}^{\rm out}$ (Å)	q	p	M (a.u.)
0.007 868	139.07	4.08	4.57	5.57	4	11	6.16

Appendix. Tight-binding scheme parameters

For completeness, we repeat the tight-binding parameters used in this study here, and refer the reader to the original paper [27] for more details. The test system was represented by a spinless s orbital tight-binding model for Au. This simple model capitalizes on the fact that the s–d orbital hybridization of Au makes its electronic structure similar to that of a rare-earth metal, with a single unpaired valence electron in the 6s orbital (there is one electron per atom). Interactions were parametrized against the cohesive energy, the structural energy difference (between fcc and bcc Au lattice geometries), the bulk modulus and the elastic constants at 0 K. The bare Hamiltonian hopping integral $H^0_{nn'}$ and the repulsive interaction $V_{nn'}$ between atoms n and n', characterized by the interatomic distance $R_{nn'}$, are respectively given below with corresponding parameters provided in table A.1:

$$H^0_{nn'} = \epsilon C/2(a/R_{nn'})^q \qquad \text{(A.1A.)}$$

$$V_{nn'} = \epsilon/2(a/R_{nn'})^p. \qquad \text{(A.2A.)}$$

Functional form interactions extend to the internal cut-off radius $r_{\rm cut}^{\rm in}$, after which they smoothly decay (via polynomial tail functions) to zero at the outer cut-off radius $r_{\rm cut}^{\rm out}$. The internal cut-off radius is located past the second-nearest neighbour in bulk Au, but in one-dimensional structures it only includes nearest neighbours. The mass M of Au was much reduced (nearing the mass of Li) in order to observe larger velocities at low temperatures. While this allowed for more atomic motion to be observed in a shorter time span, such atomic mobility is generally higher than that of real molecular systems. The total energy was evaluated using the tight-binding band model since we were concerned with differences in energy. With $\mathbf{P}_n$ and M_n as the momentum and mass of atom n, and including the charge self-consistency terms described in section 2.1, the total energy of the system was expressed as

$$\begin{aligned} E = {} & 2\mathrm{Tr}[\mathbf{\Omega H}^{\rm TB}] \\ & + \tfrac{1}{2}\sum_n \Delta q_n \left(U_n \Delta q_n + \sum_{n' \neq n} u_{nn'} \Delta q'_n / R_{nn'} \right) \\ & + \epsilon/2 \sum_n \sum_{n' \neq n} (a/R_{nn'})^p + \sum_n \mathbf{P}_n^2/2M_n. \end{aligned} \qquad \text{(A.3A.)}$$

References

[1] Donhauser Z J *et al* 2001 *Science* **292** 2303
[2] Ramachandran G K, Hopson T J, Rawlett A M, Nagahara L A, Primak A and Lindsay S M 2003 *Science* **300** 1413
[3] Chen Y, Ohlberg D A A, Li X, Stewart D R, Williams R S, Jeppesen J O, Nielsen K A, Stoddart J F, Olynick D L and Anderson E 2003 *Appl. Phys. Lett.* **82** 1610
[4] Chen J, Reed M A, Rawlett A M and Tour J M 1999 *Science* **286** 1550
[5] Dadosh T, Gordin Y, Krahne R, Khivrich I, Mahalu D, Frydman V, Spreling J, Yacoby A and Bar-Joseph I 2005 *Nature* **436** 677
[6] Galperin M, Ratner M A, Nitzan A and Troisi A 2008 *Science* **319** 1056
[7] Horsfield A P, Bowler D R, Ness H, Sánchez C G, Todorov T N and Fisher A J 2006 *Rep. Prog. Phys.* **69** 1195
[8] Durkan C, Schneider M A and Welland M E 1999 *J. Appl. Phys.* **86** 1280
[9] Hoekstra J, Sutton A P, Todorov T N and Horsfield A P 2000 *Phys. Rev.* B **62** 8568
[10] Todorov T N, Hoekstra J and Sutton A P 2001 *Phys. Rev. Lett.* **86** 3606
[11] Datta S 1995 *Electronic Transport in Mesoscopic Systems* (Cambridge: Cambridge University Press) chapter 2
[12] Hall L E, Reimers J R, Hush N S and Silverbrook K 2000 *J. Chem. Phys.* **112** 1510
[13] Lee W, Jean N and Sanvito S 2009 *Phys. Rev.* B **79** 085120
[14] Car R and Parrinello M 1985 *Phys. Rev. Lett.* **55** 2471
[15] Dundas D, McEniry E J and Todorov T N 2009 *Nature Nanotechnol.* **4** 99
[16] Král P and Seideman T 2005 *J. Chem. Phys.* **123** 184702
[17] Theilhaber J 1992 *Phys. Rev.* B **46** 12990
[18] Saalmann U and Schmidt R 1998 *Phys. Rev. Lett.* **80** 3213
[19] Allen R E 1994 *Phys. Rev.* B **50** 18629
[20] Todorov T N 2001 *J. Phys.: Condens. Matter* **13** 10125
[21] Todorov T N 2002 *J. Phys.: Condens. Matter* **14** 3049
[22] Verdozzi C, Stefanucci G and Almbladh C O 2006 *Phys. Rev. Lett.* **97** 046603
[23] Vignale G, Ullrich C A and Conti S 1997 *Phys. Rev. Lett.* **79** 4878
[24] Sánchez C G, Stamenova M, Sanvito S, Bowler D R, Horsfield A P and Todorov T N 2006 *J. Chem. Phys.* **124** 214708
[25] Todorov T N, Hoekstra J and Sutton A P 2000 *Phil. Mag.* B **80** 421
[26] Shah M and Pettifor D G 1993 *J. Alloys Compounds* **197** 145
[27] Sutton A P, Todorov T N, Cawkwell M J and Hoekstra J 2001 *Phil. Mag.* A **81** 1833
[28] Hellmann H 1937 *Einführing in die Quantenchemie* (Leipzig: Franz Deuticke)
[29] Pulay P 1969 *Mol. Phys.* **17** 197
[30] Di Ventra M and Pantelides S T 2000 *Phys. Rev.* B **61** 16207
[31] Sutton A P and Todorov T N 2004 *Mol. Phys.* **102** 919
[32] Tully J C 1990 *J. Chem. Phys.* **93** 1061
[33] Jasper A W and Truhlar D G 2005 *J. Chem. Phys.* **122** 044101
[34] Montgomery M J, Todorov T N and Sutton A P 2002 *J. Phys.: Condens. Matter* **14** 5377
[35] Horsfield A P, Bowler D R, Fisher A J, Todorov T N and Montgomery M J 2004 *J. Phys.: Condens. Matter* **16** 3609
[36] Di Ventra M, Kim S G, Pantelides S T and Lang N D 2001 *Phys. Rev. Lett.* **86** 288
[37] Chen J and Reed M A 2002 *Chem. Phys.* **281** 127
[38] Horsfield A P, Bowler D R, Fisher A J, Todorov T N and Sánchez C G 2005 *J. Phys.: Condens. Matter* **17** 4793
[39] Pettifor D G 1995 *Bonding and Structure of Molecules and Solids* (Oxford: Oxford University Press) chapter 4